

## SUPPORTING INFORMATION:

### Experimental and Theoretical Investigation of Benzothiazole Oxidation by OH in Air and the Role of O<sub>2</sub>

Natalia V. Karimova<sup>1</sup>, Weihong Wang<sup>1</sup>, R. Benny Gerber<sup>1,2,\*</sup>, Barbara J. Finlayson-Pitts<sup>1,\*</sup>

<sup>1</sup>Department of Chemistry, University of California Irvine, CA 92697, USA

<sup>2</sup>The Institute of Chemistry and Fritz Haber Research Center, The Hebrew University of Jerusalem,  
91904 Jerusalem, Israel

\* Corresponding author - experiment: Barbara J. Finlayson-Pitts, [bjfinlay@uci.edu](mailto:bjfinlay@uci.edu)

\* Corresponding author - theory: R. Benny Gerber, [bgerber@uci.edu](mailto:bgerber@uci.edu)

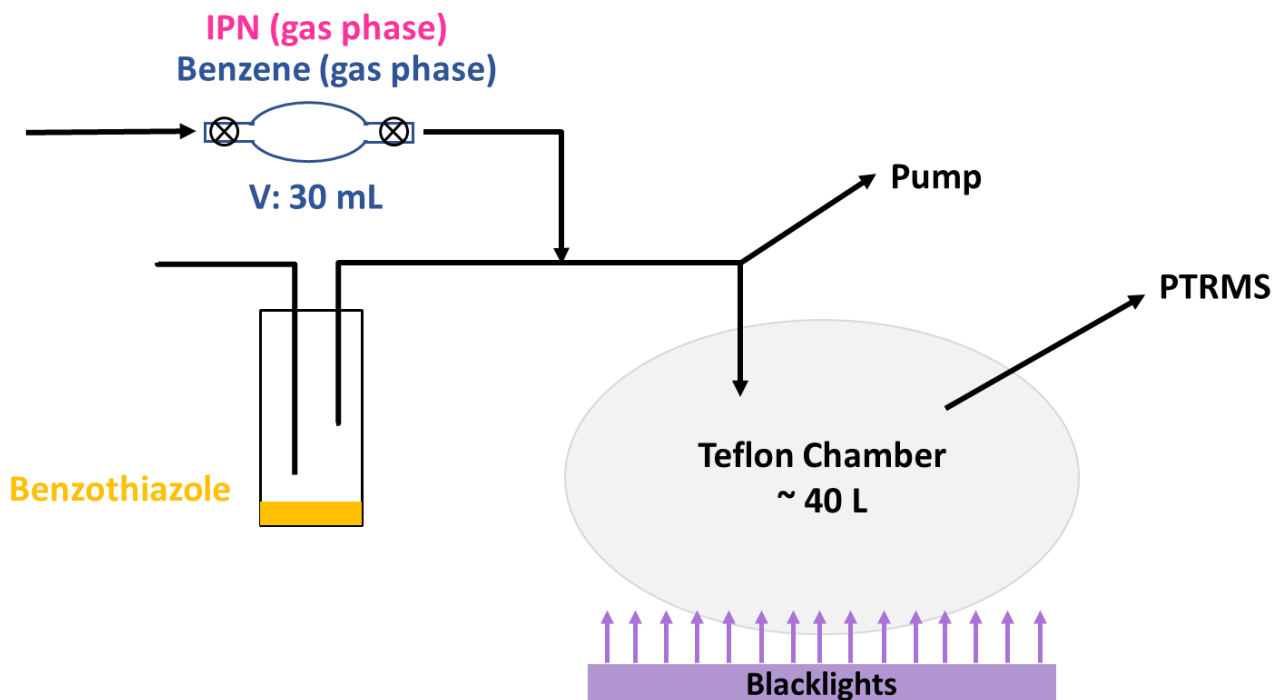


**Figure S1.** Experimental apparatus for OH-BTH reaction.

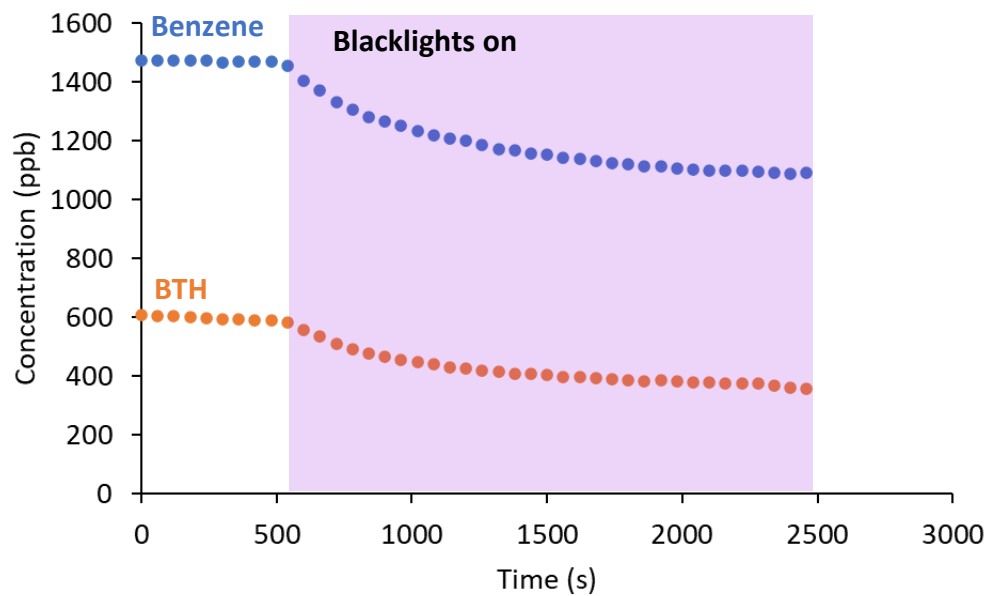


**Figure S2.** Typical time profile for BTH and benzene before and during photolysis.

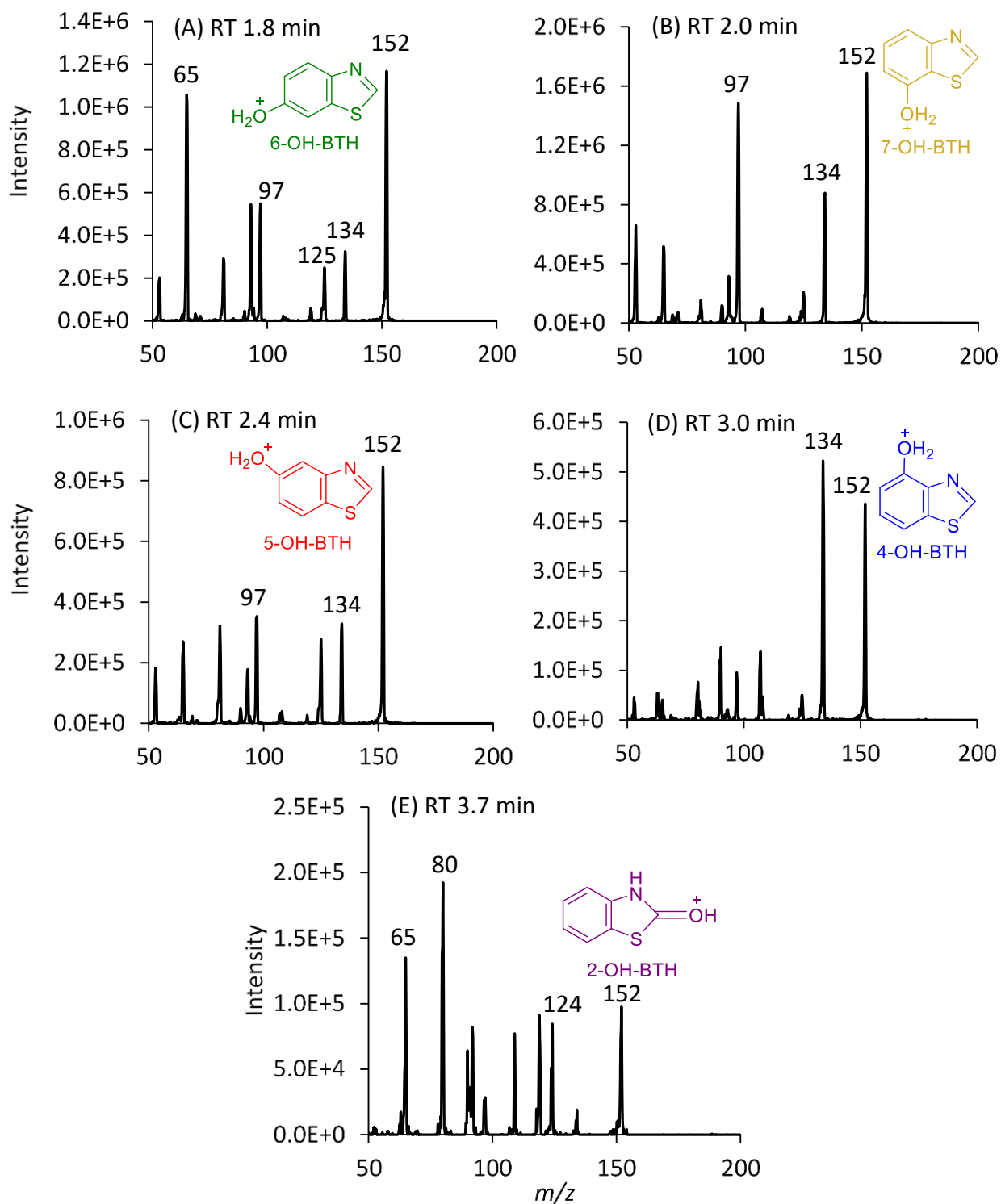


**Figure S3.** MS/MS spectra of BTH-OH reaction products for  $m/z$  152 at 25 eV collision energy at different retention times (RT) from TQD and their structures identified by comparison with standards.

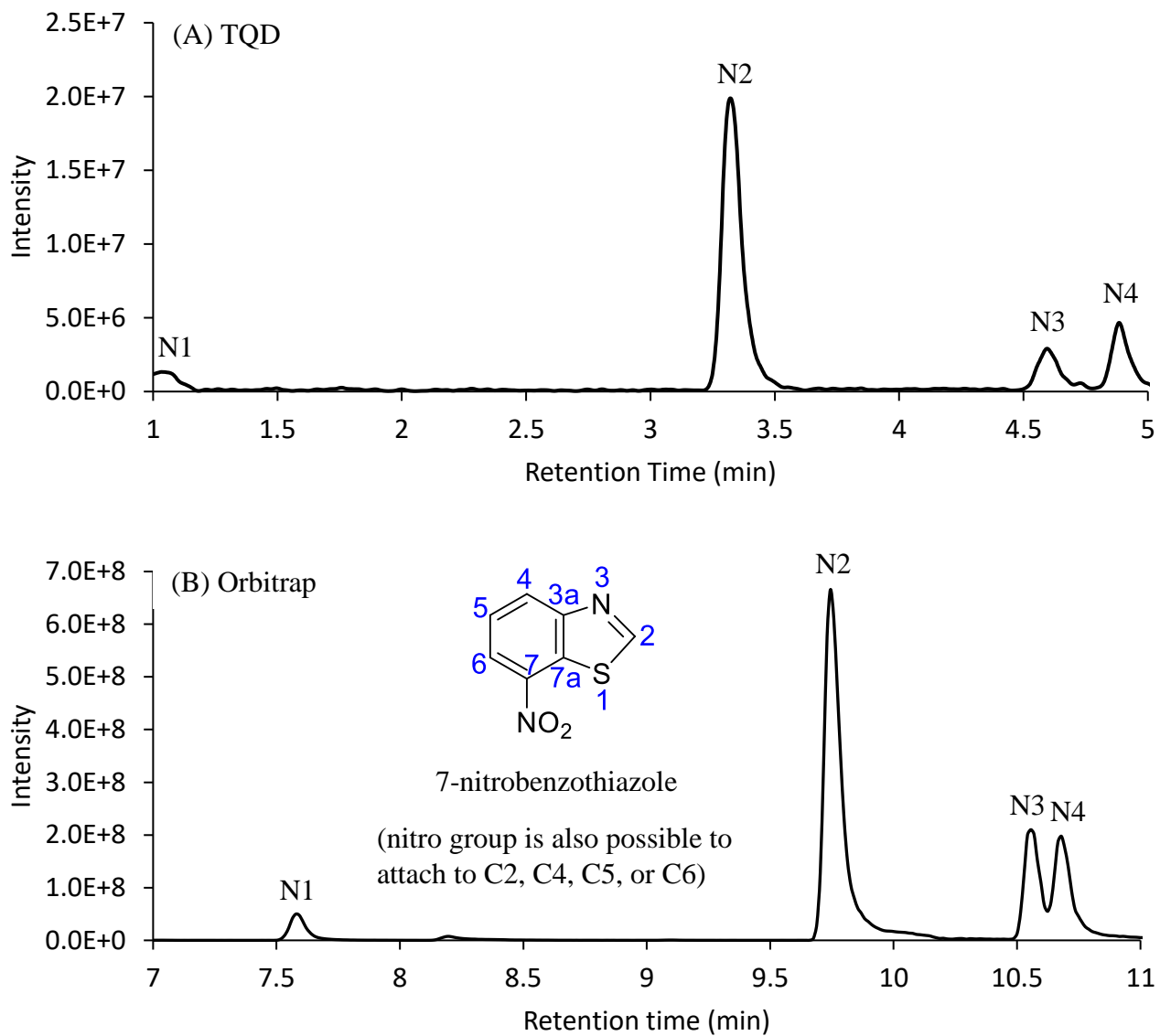


**Figure S4.** Extracted ion chromatograms at  $m/z$  181 of four products from BTH-OH reaction ( $C_4H_7N_2O_2SH^+$ , nitrobenzothiazole isomers N1, N2, N3 and N4) from (A) TQD and (B) Orbitrap.

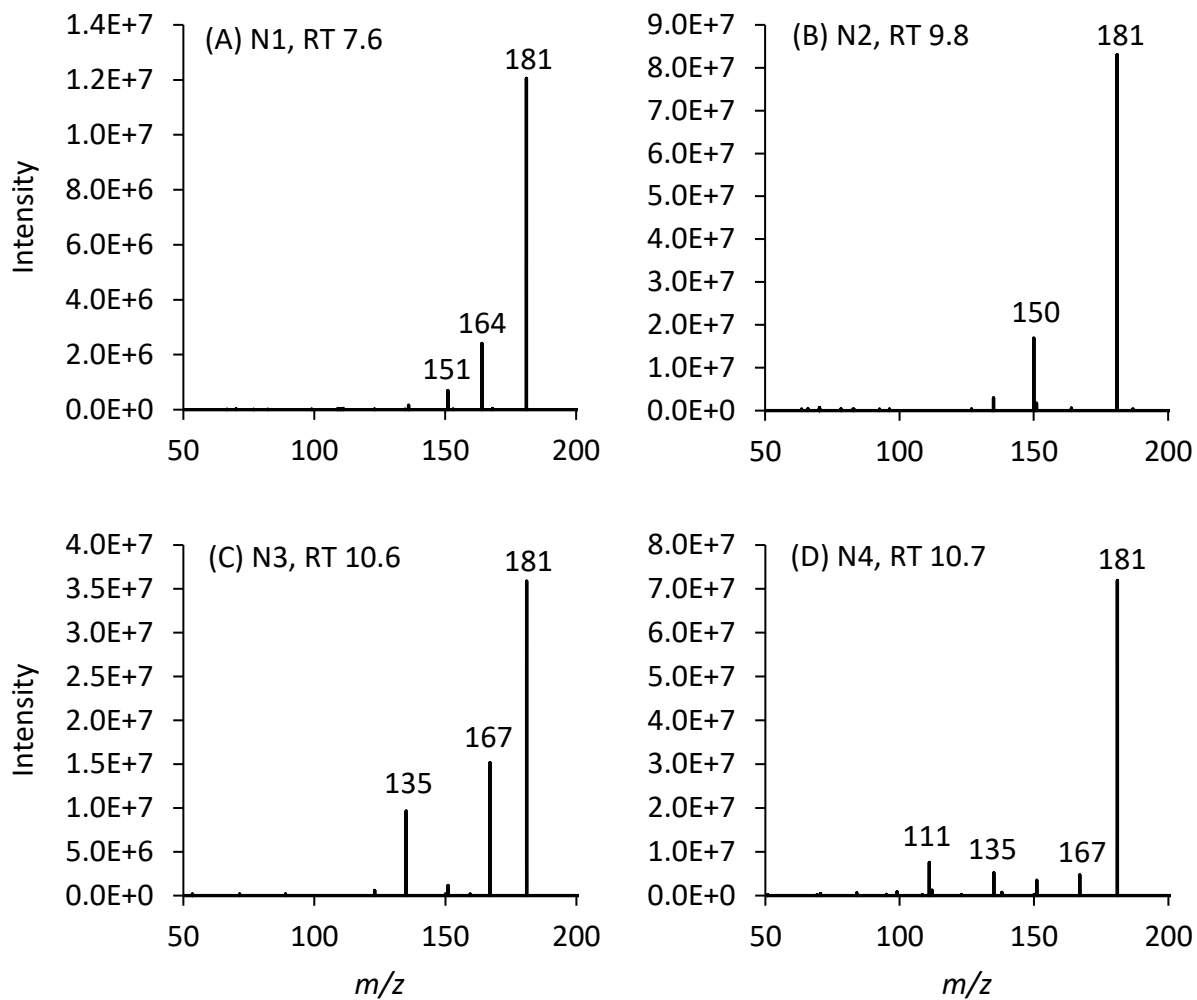


**Figure S5.** MS/MS spectra for  $m/z$  181 at different retention times (RT) from Orbitrap. N1, N2, N3 and N4 are nitrobenzothiazole isomers from **Fig. S4**.

### Text S1: DFT vs. CDFT

For systems with an oxygen molecule in the doublet state, the DFT method predicted the  $S^2 = S(S + 1)$  value incorrectly: ideally,  $S^2$  of doublet should be close to 0.75 but instead returned a value of 1.6900, suggesting a hybrid state between doublet and triplet. We tested several DFT functionals such as M06-2X, CAM-B3LYP, B3LYP and advanced methods like CCSD(T) and ADC(n) for  $n = 0$  to 3, and none could accurately predict the correct  $S^2$  value for these systems. Unlike the quartet state calculations, those in the doublet state consistently presented discrepancies with  $S^2$ . Therefore, we considered an alternative approach, constrained density functional theory (CDFT) where spin contamination is explicitly controlled.<sup>37-38</sup> Application of CDFT<sup>39</sup> allowed us to address the spin issue for systems in a doublet state with an oxygen molecule. This method was used consistently for every molecule and complex we simulated. **Table S1** lists the charges, multiplicities, and spin constraints for each system type used in these calculations.

The geometries of stationary points and activation barriers obtained with DFT and CDFT are compared in **Tables S2-S5**. Both DFT and CDFT yield identical structures with maximum distance differences capped at 0.03 Å. Relative energy comparisons on the potential energy surface (PES) demonstrate a reasonable consensus between the methods. However, CDFT slightly underperforms in complex stabilization due to constraints on electron density, with the most notable energy difference between DFT and CDFT being 0.3 kcal/mol. A particular challenge arose with the localization of the C6 pre-reaction complex (n-BTH...OH (**1**)) using CDFT, where the structure consistently moves to the C7 configuration, the more stable isomer. This issue, which was not encountered with DFT, underscores a potential limitation of the CDFT approach when using the BECKE\_SHIFT set to UNSHIFTED. When the same UNSHIFTED setting was applied in DFT, a similar transition from the C6 to C7 complex was observed. This setting does not modify the exchange-correlation potential near the nucleus, which is crucial for accurately capturing electron density near regions of high electron density or near heavy atoms. In our tests, changing this setting in CDFT led to structural collapses, hence the necessity to maintain it UNSHIFTED. Apart from the C6 issue with pre-reaction complex in CDFT, all other structures were consistently stabilized across both methods, as confirmed in **Tables S3-S5**. Overall, this comparative analysis affirms that CDFT is quite effective for modeling interactions between the OH radical and the BTH molecule. Despite minor discrepancies in energy stabilization, the strong agreement in energy barriers and structural geometries supports the continued use of CDFT for further computational investigations of these reactions.

**Table S1.** The multiplicities and spin constraints for each system type used in CDFT calculations.

System	Charge	Multiplicity	Spin Constrained
$^3\text{O}_2$	0	3	2 unpaired electrons on $^3\text{O}_2$
OH•	0	2	1 unpaired electron on OH
BTH	0	1	0 unpaired electron on BTH
OHBTH (products)	0	1	0 unpaired electron on BTH
BTH/OH•	0	2	1 unpaired electron on OH/BTH
OHBTH•/ $^3\text{O}_2$	0	4	2 unpaired electrons on $^3\text{O}_2$ fragment 1 unpaired electron on OHBTH fragment
OHBTH/OO•	0	2	1 unpaired electron on $\text{O}_2$ fragment 0 unpaired electron on OHBTH fragment
OHBTH/HOO•	0	2	1 unpaired electron on HOO fragment 0 unpaired electron on OHBTH fragment
HOO•	0	2	1 unpaired electron on OOH

**Table S2.** Barrier ( $\Delta E$ , kcal/mol) comparison (DFT vs. CDFT) of the reaction interaction of OH radical with BTH (B3LYP-D/6-311+G\*).

	DFT	CDFT
<b>C2</b>	0.7	0.8
<b>C4</b>	0.9	1.1
<b>C5</b>	1.1	1.4
<b>C6</b>	0.8	0.9
<b>C7</b>	0.4	0.5

**Table S3.** Distances (Å) in pre-reaction complexes BTH...OH obtained using DFT and CDFT (B3LYP-D/6-311+G\*)

	C2-attack		C4-attack		C5-attack		C6-attack		C7-attack	
	DFT	CDFT								
S1-C2	1.76	1.76	1.76	1.76	1.77	1.77	1.76	—	1.76	1.76
C2-N3	1.30	1.30	1.29	1.29	1.29	1.29	1.29	—	1.29	1.29
N3-C3a	1.38	1.38	1.39	1.39	1.39	1.39	1.38	—	1.39	1.39
C3a-C7a	1.42	1.42	1.41	1.41	1.42	1.41	1.42	—	1.41	1.41
C7a-S1	1.75	1.75	1.75	1.75	1.75	1.75	1.75	—	1.75	1.74
C3a-C4	1.40	1.40	1.41	1.41	1.40	1.40	1.41	—	1.40	1.40
C4-C5	1.39	1.39	1.40	1.39	1.40	1.40	1.38	—	1.39	1.39
C5-C6	1.41	1.41	1.40	1.40	1.41	1.41	1.41	—	1.40	1.40
C6-C5	1.39	1.39	1.39	1.39	1.39	1.38	1.40	—	1.40	1.40
Cn...O	2.53	2.53	2.44	2.44	2.42	2.42	2.40	—	2.36	2.36
O-H	0.98	0.98	0.98	0.98	0.97	0.97	0.97	—	0.97	0.97
H...N3	2.47	2.47	2.95	2.93	4.09	4.09	4.62	—	4.49	4.49

**Table S4.** Distances (Å) in Transition State BTH...OH obtained using DFT and CDFT (B3LYP-D/6-311+G\*)

	C2-attack		C4-attack		C5-attack		C6-attack		C7-attack	
	DFT	CDFT								
S1-C2	1.77	1.77	1.76	1.76	1.77	1.77	1.76	1.76	1.77	1.76
C2-N3	1.32	1.32	1.29	1.29	1.29	1.28	1.29	1.29	1.29	1.29
N3-C3a	1.37	1.37	1.38	1.38	1.39	1.39	1.38	1.38	1.39	1.39
C3a-C7a	1.42	1.42	1.41	1.41	1.42	1.42	1.42	1.42	1.41	1.41
C7a-S1	1.74	1.74	1.75	1.75	1.75	1.74	1.76	1.76	1.74	1.74
C3a-C4	1.41	1.41	1.42	1.42	1.39	1.39	1.41	1.41	1.41	1.41
C4-C5	1.38	1.38	1.41	1.41	1.42	1.42	1.38	1.38	1.39	1.39
C5-C6	1.41	1.41	1.39	1.39	1.43	1.43	1.43	1.43	1.40	1.40
C6-C5	1.39	1.39	1.40	1.40	1.38	1.38	1.42	1.42	1.42	1.42
Cn...O	2.14	2.14	2.06	2.06	2.00	2.00	2.04	2.04	2.07	2.07
O-H	0.97	0.97	0.97	0.97	0.97	0.97	0.97	0.97	0.97	0.97
H...N3	2.48	2.49	2.83	2.83	4.21	4.23	4.61	4.60	4.38	4.40

**Table S5.** Distances (Å) in post-reaction complexes OHBTH radical intermediate obtained using DFT and CDFT (B3LYP-D/6-311+G\*)

	C2-attack		C4-attack		C5-attack		C6-attack		C7-attack	
	DFT	CDFT								
S1-C2	1.95	1.95	1.75	1.75	1.78	1.78	1.77	1.77	1.76	1.76
C2-N3	1.42	1.42	1.30	1.30	1.28	1.28	1.30	1.30	1.29	1.29
N3-C3a	1.32	1.32	1.36	1.36	1.40	1.40	1.36	1.36	1.39	1.39
C3a-C7a	1.45	1.45	1.39	1.39	1.42	1.42	1.43	1.43	1.39	1.39
C7a-S1	1.74	1.74	1.75	1.75	1.74	1.74	1.77	1.77	1.73	1.73
C3a-C4	1.43	1.43	1.50	1.50	1.38	1.38	1.43	1.43	1.42	1.42
C4-C5	1.38	1.38	1.50	1.50	1.50	1.50	1.35	1.35	1.41	1.41
C5-C6	1.41	1.41	1.37	1.37	1.51	1.51	1.51	1.51	1.37	1.37
C6-C5	1.39	1.39	1.42	1.42	1.36	1.36	1.50	1.50	1.51	1.51
Cn...O	1.38	1.38	1.44	1.44	1.46	1.45	1.45	1.45	1.45	1.45
O-H	0.97	0.97	0.97	0.97	0.97	0.97	0.97	0.97	0.97	0.97
H...N3	2.45	2.45	2.63	2.63	4.52	4.52	5.03	5.04	4.56	4.56

**Table S6.** (C4, C5, C6 and C7 products) Relative energies ( $\Delta E$ , kcal/mol) of the gas phase reaction OH + BTH  $\rightarrow$  OH-BTH in the presence of O<sub>2</sub> (CDFT-B2PLYP/6-311++G\*\*//B3LYP-D/6-311+G\*), and comparison of activation barriers .

<b>OH attached by</b>	<b>C4</b>		<b>C5</b>		<b>C6</b>		<b>C7</b>	
<b>O<sub>2</sub> attached by</b>	<b>C3a</b>	<b>C5</b>	<b>C6</b>	<b>C4</b>	<b>C5</b>	<b>C7</b>	<b>C7a</b>	<b>C6</b>
$\cdot\text{OH} + \text{BTH} + {}^3\text{O}_2$	0.0		0.0		0.0		0.0	
$\cdot\text{OH}\dots\text{BTH} + {}^3\text{O}_2$	-3.64		-3.78		-4.18		-4.20	
TS1	-0.4		0.0		-0.7		-2.1	
$\text{OH-BTH}\cdot + {}^3\text{O}_2$	-18.1		-12.5		-15.1		-18.0	
$\text{OH-BTH}\cdot\dots{}^3\text{O}_2$ (quartet state)	-22.3		-16.1		-18.5		-22.0	
TS2 (Q $\rightarrow$ D)	-11.7	-15.2	-7.9	-11.8	-8.8	-13.4	-10.9	-14.5
$\text{OH-BTH-OO}\cdot$ (doublet state)	-13.4	-27.2	-16.6	-28.0	-16.5	-28.2	-14.5	-26.6
TS3	-10.1	-17.7	-9.3	-15.9	-9.6	-16.8	-10.9	-16.5
$\text{OH-BTH}\dots\text{HOO}\cdot$	-52.1	-51.2	-48.5	-50.0	-49.6	-48.0	-49.3	-50.3
$\text{OH-BTH} + \text{HOO}\cdot$	-43.9	-43.9	-40.9	-40.9	-40.8	-40.8	-41.0	-41.0
<b>Comparison of the activation barriers</b>								
<b>OH attached by</b>	<b>C4</b>		<b>C5</b>		<b>C6</b>		<b>C7</b>	
<b>O<sub>2</sub> attached by</b>	<b>C3a</b>	<b>C5</b>	<b>C6</b>	<b>C4</b>	<b>C5</b>	<b>C7</b>	<b>C7a</b>	<b>C6</b>
Barrier-1	3.2		3.8		3.5		2.1	
Barrier-2	10.6	7.1	8.2	4.7	9.8	5.1	11.1	7.5
Barrier-3	3.3	9.6	7.2	12.1	6.9	11.4	3.6	10.1

**Table S7.** (C2 product) Relative energies ( $\Delta E$ , kcal/mol) of the gas phase reaction  $\text{OH} + \text{BTH} \rightarrow \text{OH-BTH}$  in the presence of  $\text{O}_2$  (CDFT-B2PLYP/6-311++G\*\*//B3LYP-D/6-311+G\*), and comparison of activation barriers .

<b>OH attached by</b>	<b>C2</b>
<b>O<sub>2</sub> coordinated by</b>	<b>N3</b>
$\cdot\text{OH} + \text{BTH} + {}^3\text{O}_2$	0.0
$\cdot\text{OH}\dots\text{BTH} + {}^3\text{O}_2$ (1')	-4.5
TS1	-1.0
$2\text{OH-BTH}\cdot + {}^3\text{O}_2$ (2')	-26.6
$2\text{OH-BTH}\cdot\dots{}^3\text{O}_2$ (3') (quartet state)	-30.7
TS2 (Q→D)	-23.4
$2\text{OH-BTH}\dots\text{OO}\cdot$ (4') (doublet state)	-21.5
TS3'	-18.6
$2\text{OH-BTH}\dots\text{OO}\cdot$ (5')	-18.1
TS4'	-18.5
$2\text{OH-BTH}\dots\text{HOO}$ (6')	-58.5
TS5'	-57.7
$2\text{OH-BTH}\dots\text{HOO}$ (7')	-66.0
TS6'	-65.5
$2(3\text{H})\text{OH-BTH}\dots\text{HOO}$ (8')	-73.5

**Table S8.** Spin density (a.u.) in the intermediate radical n-OHBTH·. Method CDFT-B3LYP-D/6-311+G\*.

<b>Atom</b>	<b>C2</b>	<b>C4</b>	<b>C5</b>	<b>C6</b>	<b>C7</b>
<b>S1</b>	0.126	0.021	0.052	0.025	0.044
<b>N3</b>	0.473	-0.061	0.056	-0.108	0.042
<b>C7a</b>	0.309	-0.125	0.422	-0.172	0.337
<b>C3a</b>	-0.176	0.272	-0.194	0.352	-0.182
<b>C7</b>	-0.110	0.564	-0.135	0.515	-0.097
<b>C4</b>	0.170	-0.103	0.509	-0.151	0.583
<b>C6</b>	0.295	-0.202	0.308	-0.042	0.513
<b>C5</b>	-0.102	0.470	-0.002	0.296	-0.221
<b>C2</b>	-0.011	0.174	-0.043	0.276	-0.040
<b>O</b>	-0.004	0.002	0.017	0.014	0.024
<b>H</b>	0.009	0.006	0.008	0.009	0.006

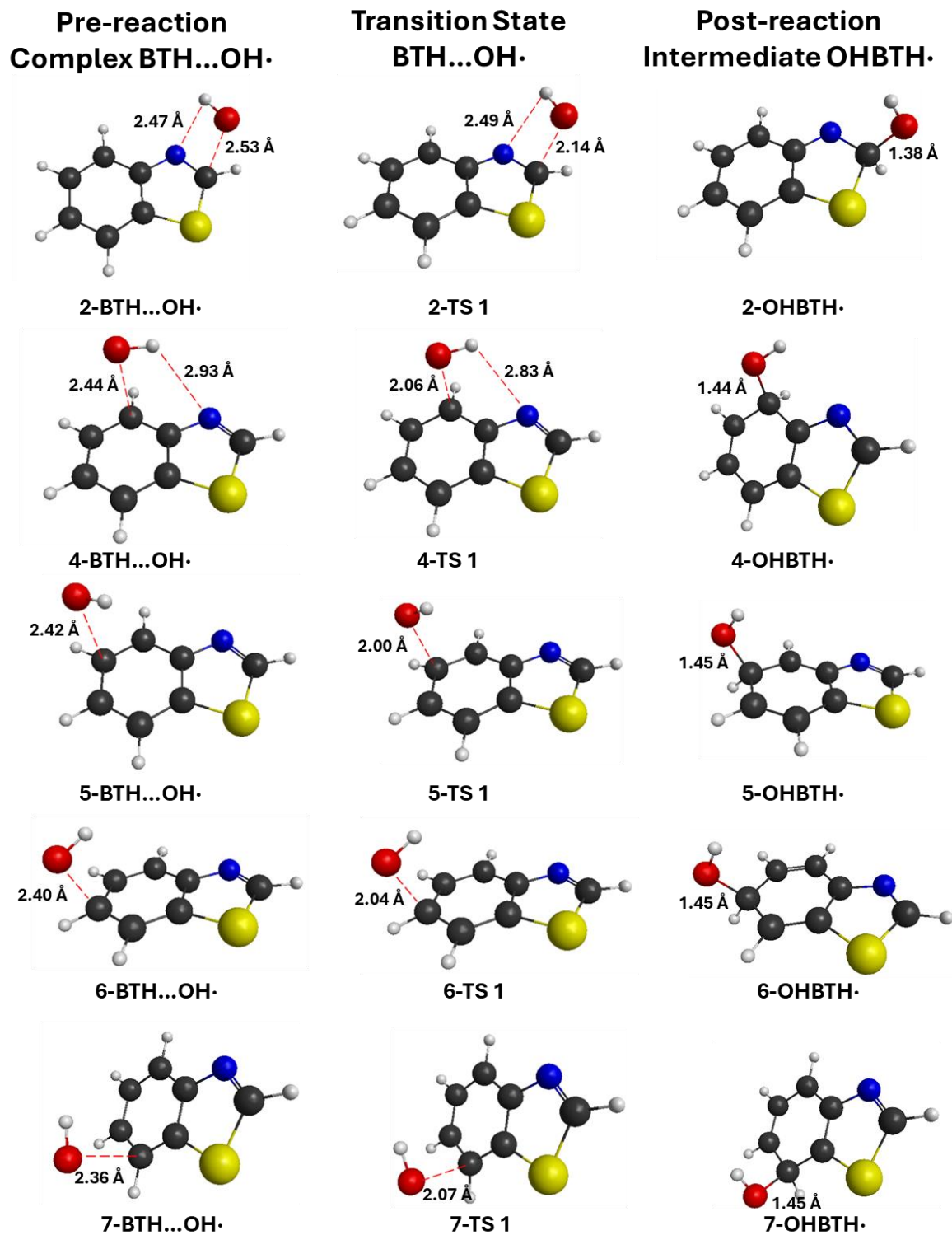


**Figure S6.** Stationary points on the PES of the reaction BTH with hydroxyl radical: OH attacks C2, C4, C5, C6, and C7 carbon atoms. The geometry optimization method is CDFT-B3LYP-D/6-311+G\*. Note: geometry of pre-reaction complex 6-BTH...OH· was obtained using unconstrained DFT and then used for calculation of CDFT energy and zero-point energy.

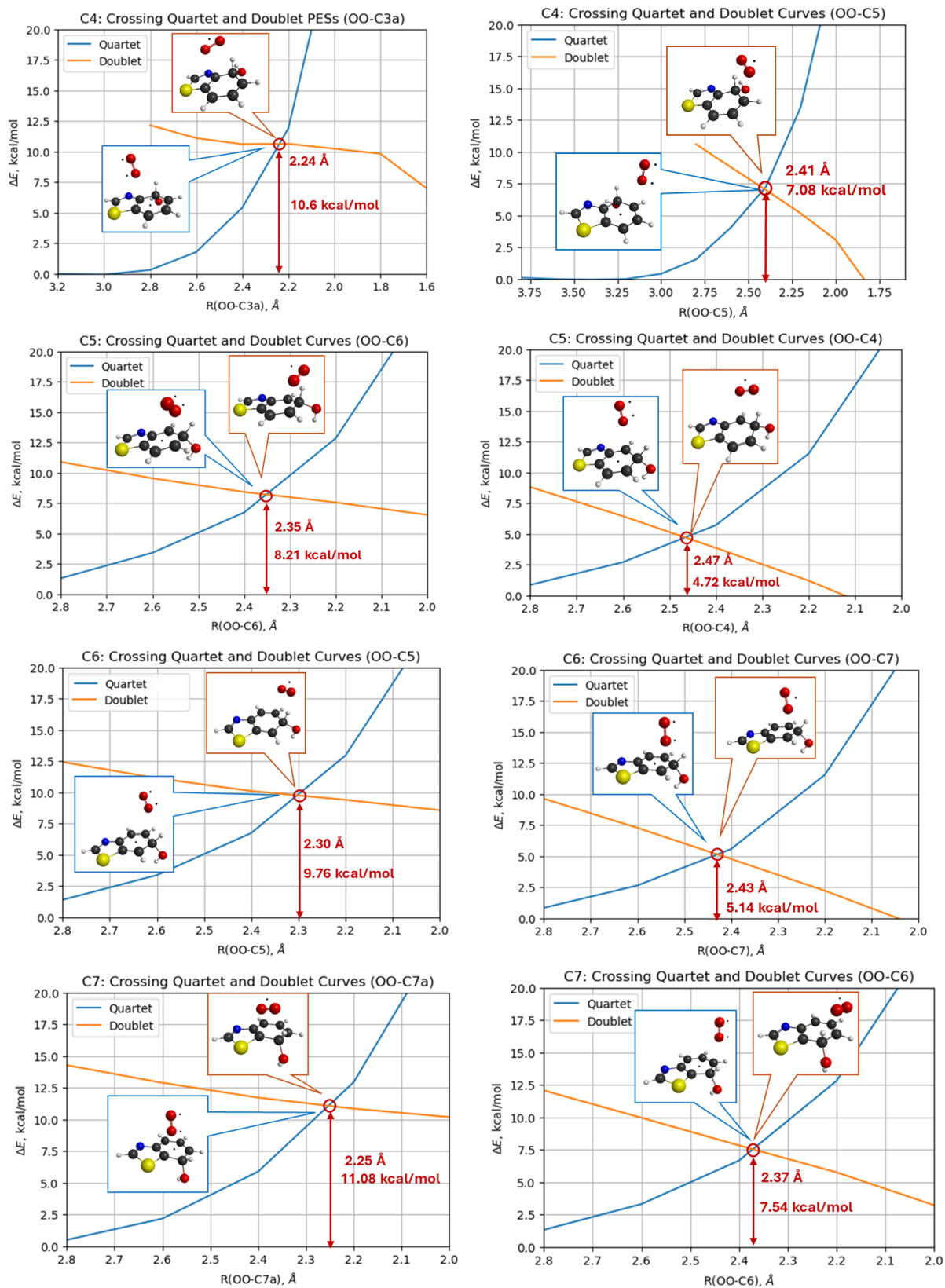


**Figure S7A.** The crossing point of quartet and doublet states:  $n$ -OHBTH·/ $^3\text{O}_2$  (three unpaired electrons, quartet state) to the  $n$ -OHBTH-OO (one unpaired electron, doublet state) for  $n = 4, 5, 6, 7$ . Approach CDFT-B2PLYP/6-311++G\*\*//B3LYP/6-311+G\*.

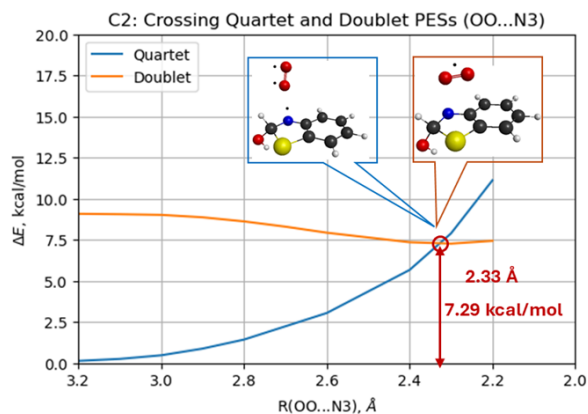


**Figure S7B.** The crossing point of quartet and doublet states:  $n\text{-OHBTH}\cdot\beta\text{O}_2$  (three unpaired electrons, quartet state) to the  $n\text{-OHBTH}\dots\text{OO}$  complex for  $n=2$ . Approach CDFT-B2PLYP/6-311++G\*\*/B3LYP/6-311+G\*.

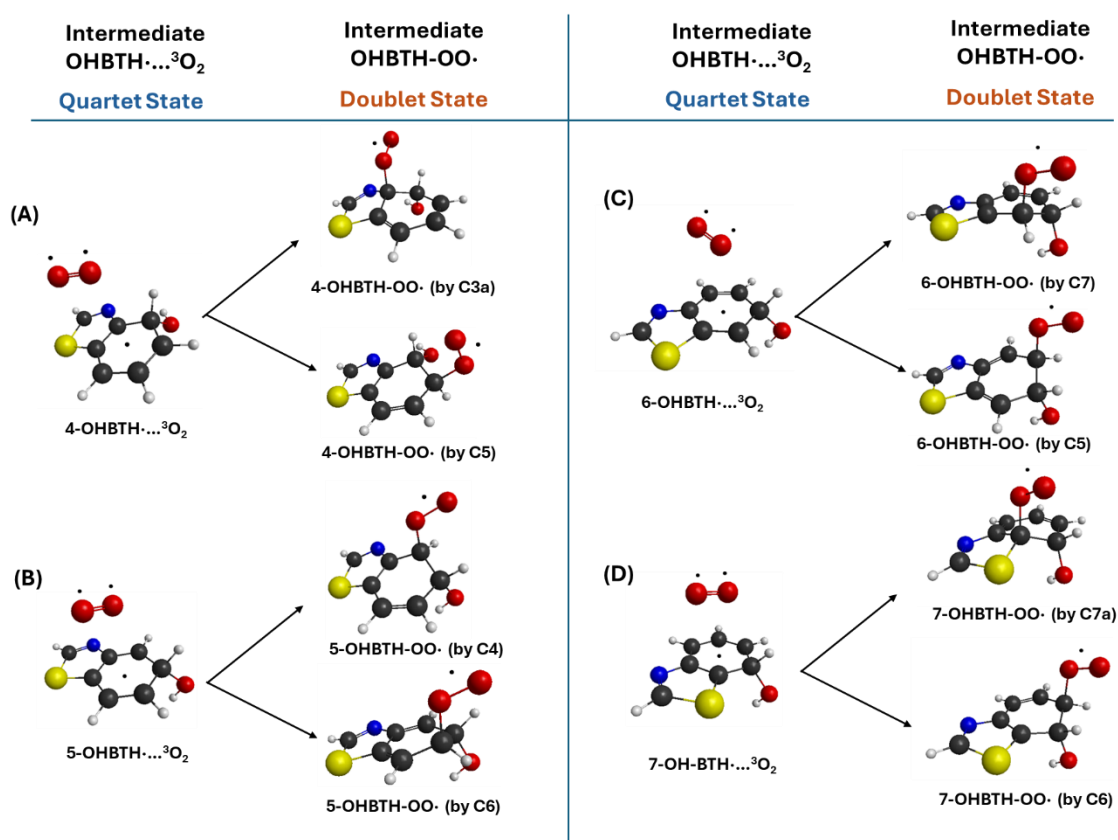


**Figure S8.** Structures of intermediates  $n\text{-OHBTH}\beta\text{O}_2$  and  $n\text{-OHBTH}\text{-OO}\cdot$ : (A) OH attacks site C4; (B) OH attacks site C5; (C) OH attacks site C6; (D) OH attacks site C7.

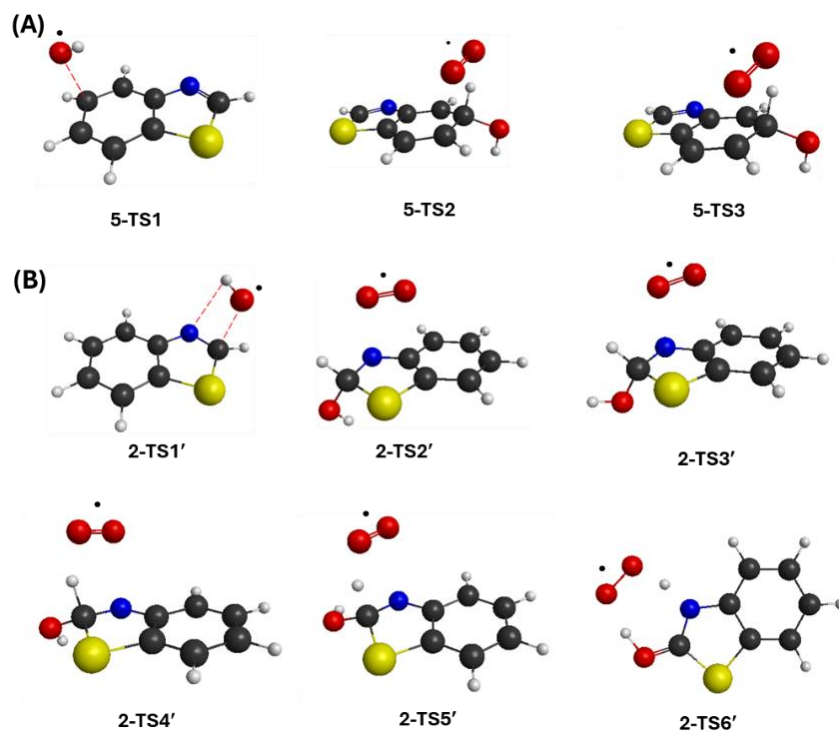


**Figure S9.** Structures of transition states from the PES of: (A) 5-OHBTH product formation; and (B) 2-OHBTH product formation. Geometry optimization method is B3LYP-D3/6-311+G\*

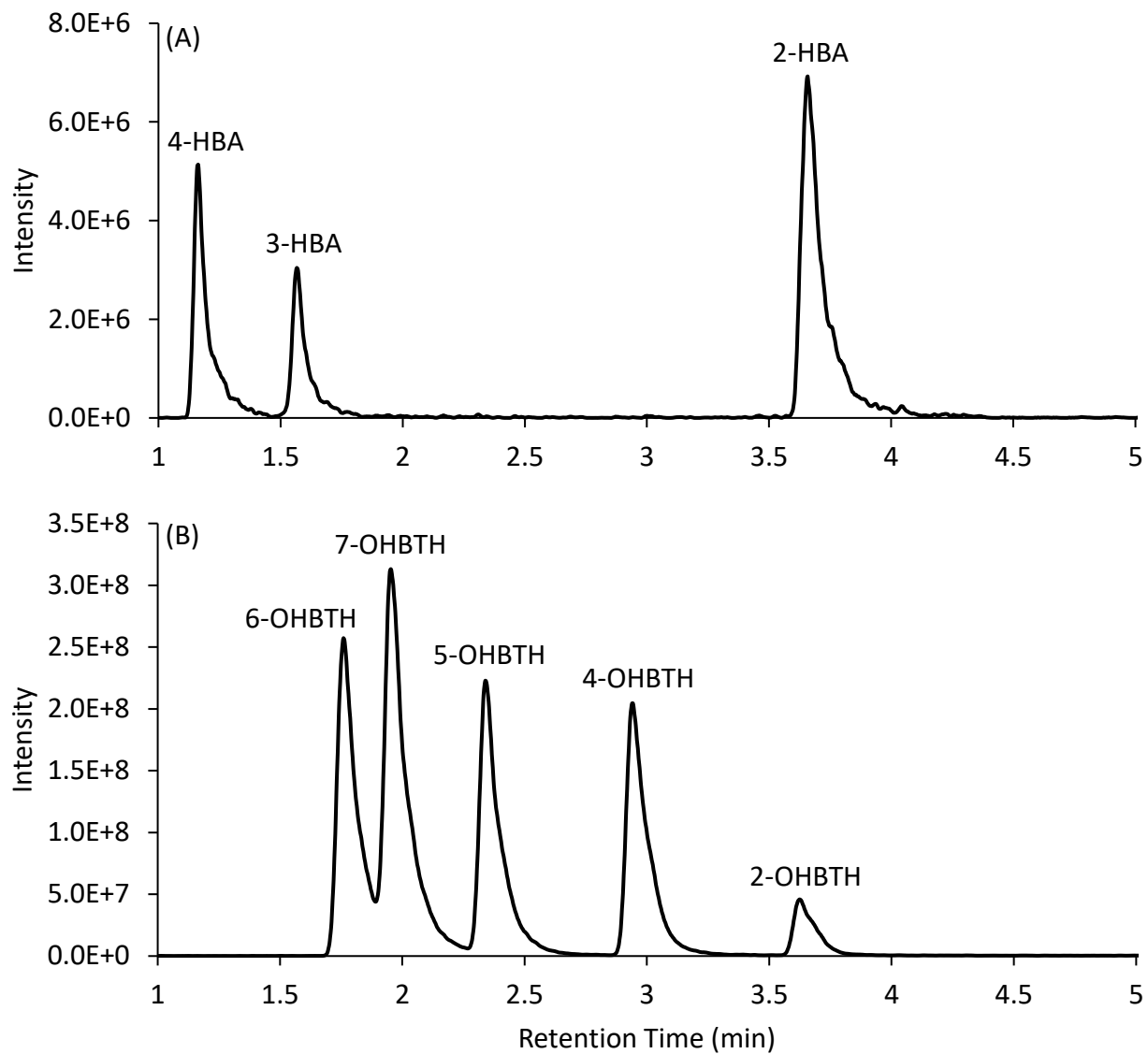


**Figure S10.** Retention times of standards of isomers of (A) 2HBA (25 mM in ACN); 3HBA (18 mM in ACN); 4HBA (18 mM in ACN); and (B) n-OHBTH (500 ng/ml each in 50:50 ACN/water).

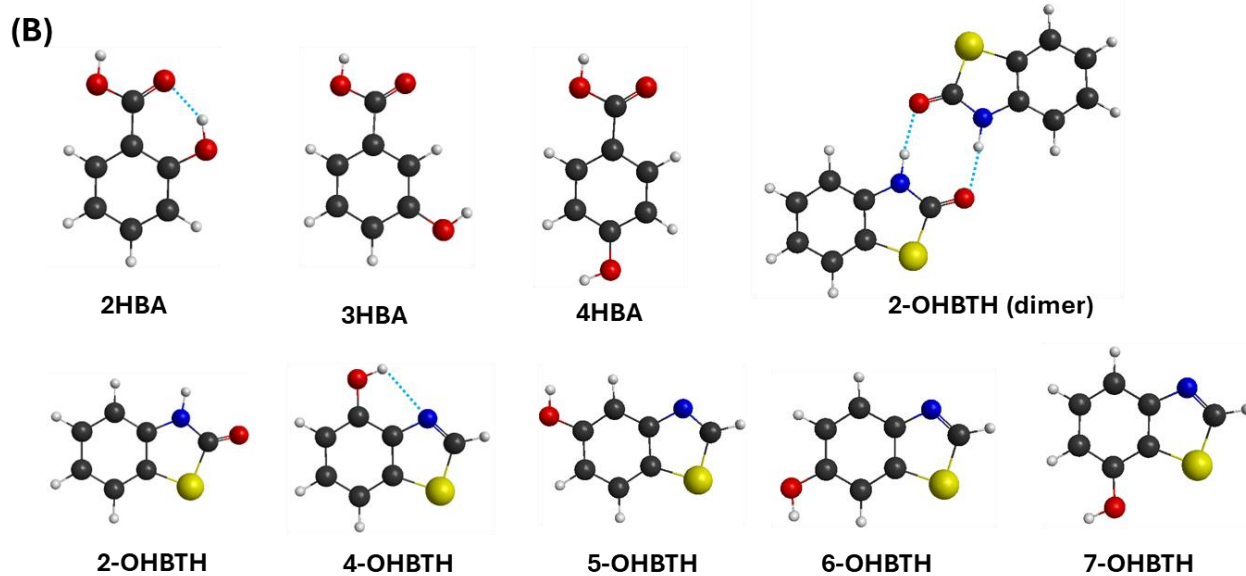
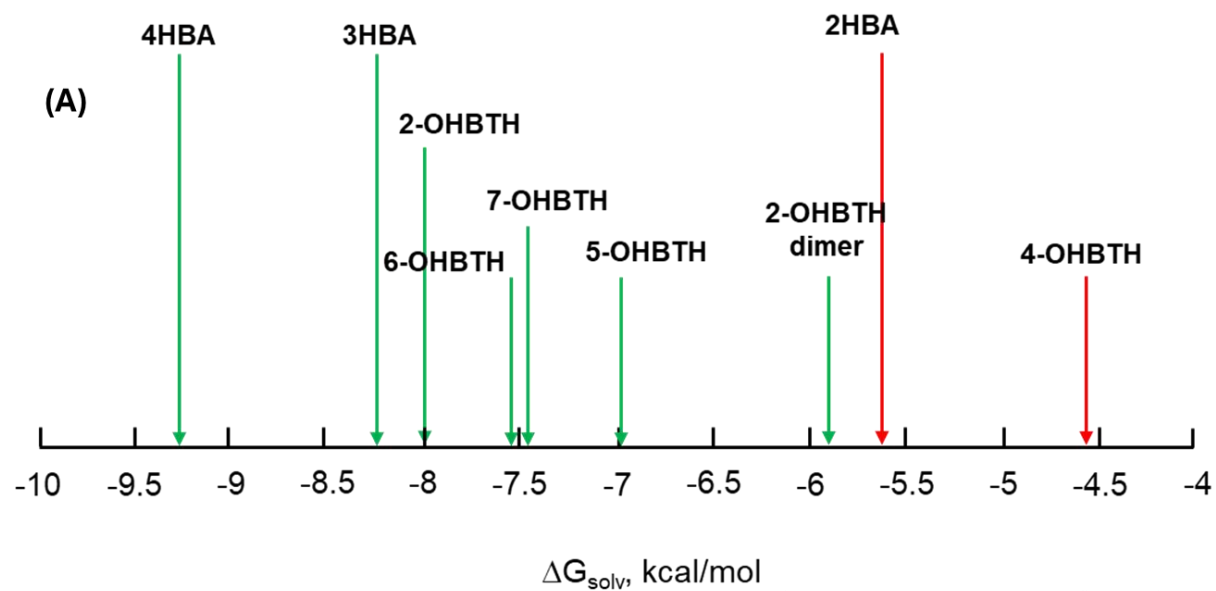


**Figure S11.** (A) Calculated solvation free energies. 2HBA and 4-OHBTH were marked in red because they have internal hydrogen bonding. (B) Structures of these HBA and n-OHBTH compounds were calculated using the IEFPCM model.